PNAS RESEARCH ARTICLE | NEUROSCIENCE

Luxotonic signals in human prefrontal cortex as a possible substrate for effects of light on mood and cognition

Shai Sabbah[a,1], Michael S. Worden[b,c], Dimitrios D. Laniado[a], David M. Berson[b,c], and Jerome N. Sanes[b,c,d,1]

Edited by Peter Strick, University of Pittsburgh Brain Institute, Pittsburgh, PA; received October 3, 2021; accepted May 16, 2022

Studies with experimental animals have revealed a mood-regulating neural pathway linking intrinsically photosensitive retinal ganglion cells (ipRGCs) and the prefrontal cortex (PFC), involved in the pathophysiology of mood disorders. Since humans also have light-intensity–encoding ipRGCs, we asked whether a similar pathway exists in humans. Here, functional MRI was used to identify PFC regions and other areas exhibiting light-intensity–dependent signals. We report 26 human brain regions having activation that either monotonically decreases or monotonically increases with light intensity. Luxotonic-related activation occurred across the cerebral cortex, in diverse subcortical structures, and in the cerebellum, encompassing regions with functions related to visual image formation, motor control, cognition, and emotion. Light suppressed PFC activation, which monotonically decreased with increasing light intensity. The sustained time course of light-evoked PFC responses and their susceptibility to prior light exposure resembled those of ipRGCs. These findings offer a functional link between light exposure and PFC-mediated cognitive and affective phenomena.

light-sensitive brain regions | fMRI | humans | frontal lobe

Significance

Humans sense changes in ambient illumination, thus luxotonic properties, unrelated to form vision, and these changes influence a wide range of functions, including circadian rhythms, visual reflexes, mood, and likely cognitive processing. While image-forming pathways in the primate brain detect minute changes in illumination, it remains unclear how light-intensity signals reach and become processed in brain structures involved in basic moods and their dysfunction, pathways that likely derive from intrinsically photosensitive retinal ganglion cells. Here, we show that prefrontal regions in the human brain have luxotonic signals. These signals have properties similar to intrinsically photosensitive retinal ganglion cells, and they may underlie light-intensity effects on complex behaviors.

Light impacts mood and cognition in humans and animals. Abnormal lighting induces depression (1–3), while bright light enhances antidepressant therapies and ameliorates both seasonal and nonseasonal depression (4–7). Bright light also affects decision-making and working memory, two key functions of the prefrontal cortex (PFC) (8–11). These light-related effects likely depend upon a specialized output channel of the retina dedicated to a stable representation of environmental illumination: that is, a light-intensity (irradiance) signal (12–14). However, the origin of the specific light-intensity signal acting in the PFC has yet to be identified. One light-intensity signal discovered in recent years, arises from intrinsically photosensitive retinal ganglion cells (ipRGCs), a rare class of retinal output neurons found both in humans and mice, among other species, with autonomous sensitivity to light by virtue of their expression of the photopigment melanopsin (15, 16). Light-intensity signals from ipRGCs are conveyed to a myriad of brain regions and affect in mice, among other functions, circadian clock photoentrainment, pupil constriction, neuroendocrine rhythms regulation, learning, and mood (17–19).

In mice, a light-intensity signal derived from ipRGCs are routed to the PFC by a remarkably direct pathway that affects mood, presumably through light-dependent modulation of PFC activity (20). Specifically, light-intensity–encoding ipRGCs innervate the perihabenular nucleus (PHb), a small region in the dorsomedial thalamus. The PHb projects in turn to the medial PFC (mPFC), a region with known roles in mood regulation (21, 22). Continuous activation of this retino-thalamo-frontocortical pathway induced depression-like behaviors in mice, while suppressing its activity protected against the negative mood effects of unnatural day–night cycles (20). This pathway is a tiny offshoot of the retino-thalamic pathway, dramatically different in scale and function from the lemniscal visual pathway through the dorsal lateral geniculate nucleus (dLGN) to the visual cortex. Notably, the PHb also projects to the nucleus accumbens (NAc), which modulates hedonic behaviors (23), and to the dorsomedial striatum, where activity is related to goal-directed actions (24). Neurons in the PHb's dorsal and ventral sectors project to the NAc and mPFC, respectively (23), and the two sectors also differ in their function: the activity of NAc-projecting neurons is gated according to the circadian rhythm, while the mPFC-projecting neurons do not express such gating.

Might a similar retino-PFC pathway link light and mood in humans? Certainly, the retinal elements exist, since light-intensity coding ipRGCs closely resembling those in mice exist in primates, including humans (25). Human studies likewise link the PFC, light exposure (5, 6), and mood (26–32) with the development of depression, and other mood disorders are likely affected by PFC dysfunction (33–36). However, the ability of the human PFC to encode light intensity remains unclear. Identifying such a pathway and understanding its function might directly promote development of

Author affiliations: [a]Department of Medical Neurobiology, Faculty of Medicine, Hebrew University of Jerusalem, Jerusalem 9112102, Israel; [b]Department of Neuroscience, Brown University, Providence, RI 02912; [c]Carney Institute for Brain Science, Brown University, Providence, RI 02912; and [d]Center for Neurorestoration and Neurotechnology, Veterans Affairs Providence Healthcare System, Providence, RI 02908

Author contributions: S.S., M.S.W., D.M.B., and J.N.S. designed research; S.S. and M.S.W. performed research; D.D.L. helped with literature searches; S.S., M.S.W., D.D.L., and J.N.S. analyzed data; and S.S., M.S.W., D.M.B., and J.N.S. wrote the paper.

The authors declare no competing interest.

This article is a PNAS Direct Submission.

[1]To whom correspondence may be addressed. Email: shai.sabbah@mail.huji.ac.il or jerome_sanes@brown.edu.

This article contains supporting information online at http://www.pnas.org/lookup/suppl/doi:10.1073/pnas.2118192119/-/DCSupplemental.

Published July 6, 2022.

approaches to treat depression, either by pharmacological manipulation of activation in selected nodes of the pathway or environmental manipulation with targeted bright-light therapy.

Here, as a first step to probe for a retinal-thalamic-frontocortical pathway in humans, we tested the hypothesis that the intensity of light reaching the eyes—stripped of color, form, and movement information—would modulate activation in the human PFC. We used functional MRI (fMRI) to identify brain regions having light-intensity–dependent activation (hereafter "luxotonic regions") and analyzed the data to identify transient and persistent activation modulation. Ten brain regions showed a steady-state activation pattern related to light intensity. Most of these regions were in the PFC or in the classic thalamocortical visual pathway; others were found in the cerebellum and a region encompassing the pineal body. The PFC regions and the pineal body exhibited marked suppression of fMRI signals by bright sustained light, while the other regions exhibited pronounced activation. The sustained time course of the light-evoked responses in the PFC resembled those of ipRGCs, and prior light exposure influenced the PFC response to light. We also found 16 regions that exhibited transient responses to changes in light intensity. These regions were located across the cerebral cortex, with functions related to visual perception, motor control, and cognition.

Results

To determine whether a light-intensity–encoding pathway modulates the human PFC, we used blood-oxygen level-dependent (BOLD) fMRI (3T Siemens Prisma, 2-mm isotropic voxels) to explore whole-brain activation patterns in 20 healthy adults who viewed full-field diffused white light stimuli. Every 30 s, the light was stepped to a new intensity drawn from one of four values, which together spanned nearly four orders of magnitude (average irradiance across the 400- to 700-nm human visible spectrum, 10.2, 12.1, 13.1, and 13.8 log photons cm^{-2} s^{-1}). All four light intensities were tested three times in each 6-min run, and each session included five runs, providing 15 total blocks at each light intensity (see *Materials and Methods* and *SI Appendix, Supplementary Materials and Methods* and Fig. S1 *A* and *B* for additional details). Participants donned Teflon goggles that diffused the light and removed any spatial contrast, as confirmed by each participant. We encouraged alertness in the participants by asking them to keep their eyes open throughout the experiment, and by requiring them to discriminate between two randomly presented tones by pressing one of two buttons (*SI Appendix*, Fig. S1*A*). We used a combination of criteria (monotonic contrast, voxel-wise threshold $P < 0.001$, cluster false-discovery rate = 0.05, cluster size > 26 voxels) to reveal brain regions that exhibited activation varying monotonically with light intensity and showing either a sustained or transient component (*SI Appendix*, Fig. S1 *C* and *D*).

Light Intensity Modulates Steady-State Activation of Diverse Cortical, Subcortical, and Cerebellar Regions. Throughout this report, we refer to brain regions exhibiting light-intensity–dependent monotonic activation as luxotonic regions, regardless of whether the response persisted throughout the 30-s period or did not. Overall, 10 brain regions met the criteria for light-intensity–dependent monotonic activation, with a significant sustained component (Fig. 1*A* and *SI Appendix*, Table S1; see *Materials and Methods* and

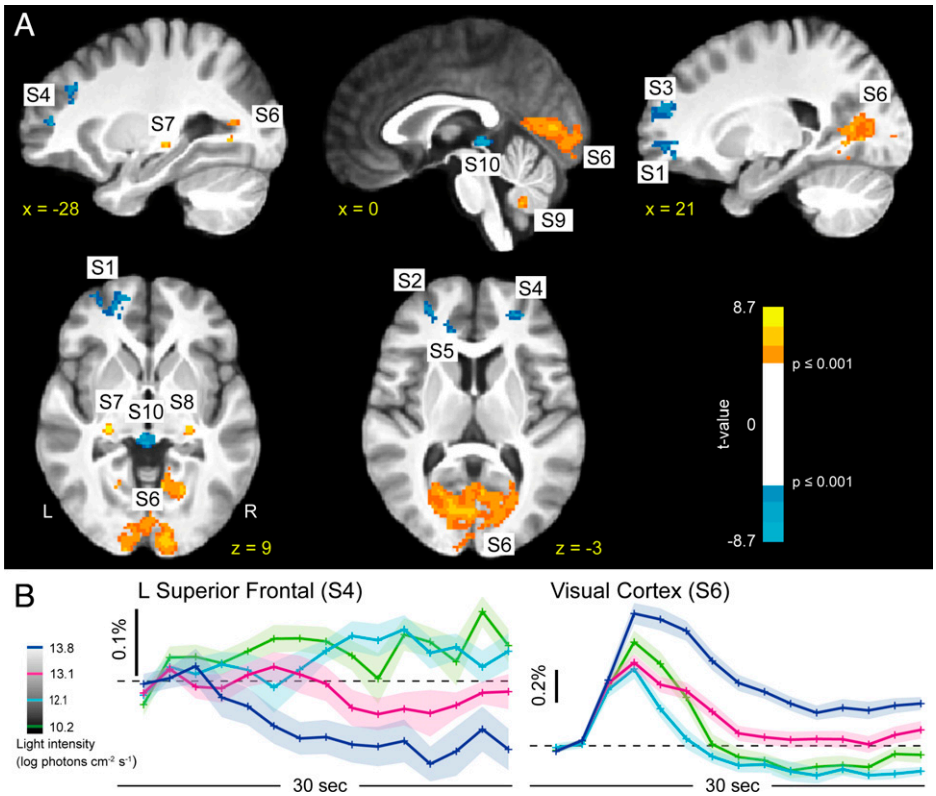

Fig. 1. Cortical, subcortical, and cerebellar luxotonic regions showing a sustained component. (*A*) The 10 identified luxotonic regions are color-coded based on the contrast for monotonic increases or decreases as a function of light intensity. The MNI coordinates of presented slices are indicated in yellow. Color scale corresponds to *t* values: warm colors (positive *t*) represent light-evoked responses increases with light intensity; cool colors (negative *t*) depict light-evoked responses decreases with light intensity. Color bar, *t* values range ±8.7, and images are thresholded at $P < 0.001$, two-tailed $t_{19} = 3.621$ (white horizontal lines). Anatomical underlay represents the mean of all 20 participants following spatial alignment. (*B*) BOLD (mean ± SEM) responses for S4 and S6 over the 30-s light stimulus, for four light intensities (given in log photons cm^{-2} s^{-1}). Data for all luxotonic regions are shown in *SI Appendix*, Fig. S2.

SI Appendix for details on the regressor used for this analysis). Light-intensity–dependent activation in all these regions persisted throughout the 30-s duration of the stimulus. In several of the regions, activation also changed abruptly upon light onset (Fig. 1*B* and *SI Appendix*, Fig. S2). Steady-state BOLD signals in those 10 brain areas with a sustained component either monotonically increased or decreased with light intensity. Five of these regions were in the PFC, specifically in the superior PFC, orbital frontal cortex (OFC), and anterior cingulate cortices (ACC, regions S1 to S5), all showing a monotonically decreasing response to increasing light intensity. In contrast, monotonically increasing responses to increasing light intensity were observed in the image-forming visual system: light intensity strongly increased the BOLD signal in the occipital lobe (S6), especially in the primary visual cortex (V1), but also in several extrastriate regions beyond V1. These results are consistent with previous studies (37–39; but see ref. 40). The dLGN (S7, S8), the thalamic relay nucleus of the primary visual pathway, is almost certainly the source of this luxotonic signal in V1, since it too exhibited bilateral, strong BOLD activation responses to bright light, that monotonically increased with light intensity. The only brain region beyond the primary visual pathway that shared the visual system's BOLD activation to light was a small region in the uvula at the inferior vermis of the cerebellum (S9). An additional small region exhibited suppressed BOLD responses that monotonically decreased with light intensity, like those in the PFC. This was a region encompassing the pineal body (S10), in which activity is known to be depressed in response to light through the influence of ipRGCs (41).

Sensitivity, calculated as the difference in steady-state response between the second lowest and highest stimulus light intensity divided by the change in intensity, was significantly larger in cortical (0.18 ± 0.06 BOLD response; mean ± SD) compared to subcortical regions (0.04 ± 0.03 BOLD response; permutation *t* test, $P = 0.005$) (*SI Appendix*, Fig. S2*B*). Between-subject variation in the time-course and response amplitude is a well-known characteristic of fMRI data, even for robust effects. Nonetheless, effects similar to those identified in the responses averaged across participants were readily detected also at the level of individual participants (*SI Appendix*, Fig. S3).

Functional Connectivity between Luxotonic Sustained Regions. We next assessed to what extent the activated regions formed independent or dependent networks, by measuring functional connectivity (Pearson correlation) between each of the 10 regions that exhibited sustained light-intensity–dependent activation (Fig. 2*A*). Note that rather than implying node-to-node interconnectivity, functional connectivity merely suggests that different patterns of correlation in the response hint to the existence of different networks. BOLD time series in luxotonic regions in the PFC generally exhibited significant positive correlations with one another (Fig. 2*A*, hot colors and red dots), except for the right ACC, in which activity correlated only with that in the right OFC. Similarly, we found positive correlations in the BOLD time series among several regions along the thalamo-visuocortical pathway: V1 (with extra striate areas) and LGN, as well as a region in the vermis of the cerebellum (BOLD time-series in V1, left LGN, and cerebellar vermis correlated positively). These BOLD time-series were either not correlated or negatively correlated with PFC regions (Fig. 2*A*, cold colors). BOLD time series in the pineal did not correlate with either the PFC group or thalamo-visuocortical pathway. Thus, it seems that sustained light intensity-dependent responses engaged two main separate functional networks, one encompassing the thalamo-visuocortical pathway and another including a set of PFC regions. The latter set of regions has been previously implicated in mood regulation and high-level cognition and value-related judgments (8–11).

Activation in Luxotonic Sustained Regions Diverges in Temporal Profile and Polarity. Our findings represent a demonstration that the PFC and the cerebellar inferior vermis and pineal body, exhibit activation modulation in proportion to light intensity. To assess the timing of the sustained light-evoked BOLD responses, we compared normalized the amplitude of all observed time courses to range between 0 and 1 (or −1) (Fig. 2*B*). Luxotonic regions in the visual cortex, LGN, and cerebellum, in which light enhanced the BOLD signal, showed a relatively rapid increase in activation (latency of ∼10 s), which then gradually declined in magnitude (Fig. 2*B*, blue, cyan, and magenta lines); this time course has consistency with the slow

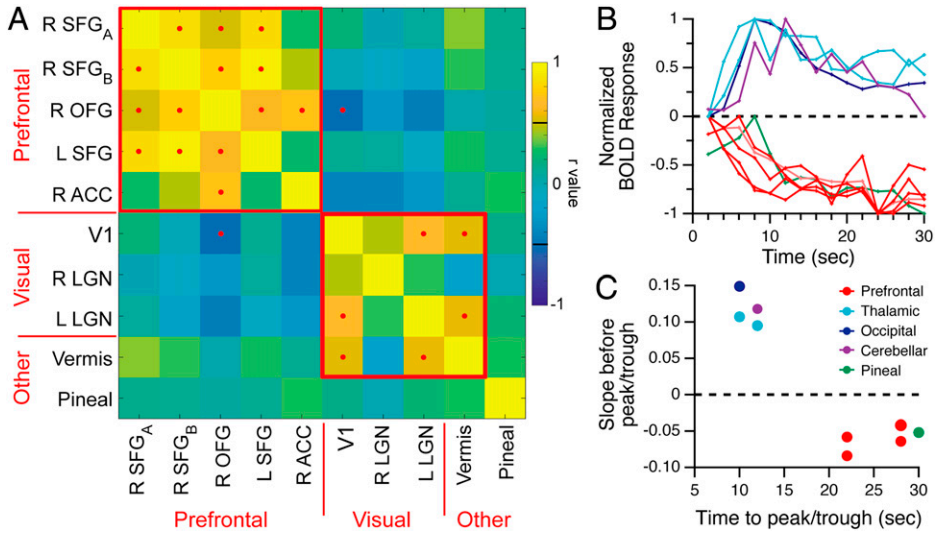

Fig. 2. Light-evoked responses with a significant sustained component are either rapid and increasing with light intensity or slow and decreasing with light intensity. (*A*) Pair-wise Pearson correlation between the 10 identified luxotonic regions. Regions are grouped as "prefrontal," "thalamo-visuocortical," and "other." Correlation coefficient of ±0.51 corresponds to a significance level of 0.05 (marked with red dots on the correlation matrix and indicated on the color scale bar). (*B*) Light-evoked responses, normalized in all 10 identified luxotonic regions to the highest light intensity, averaged across 20 participants, fell into two functional groups: rapid and slow. Responses are color-coded based on the general brain region, as depicted in the legend at the bottom. (*C*) Distribution of the 10 identified luxotonic regions as a function of the slope before peak/trough and the time to peak/trough. Responses are color-coded based on the general brain region.

BOLD response to transient stimulation. In contrast, activity in all the PFC luxotonic regions and pineal body dropped below baseline, reaching its minimum toward the end of the 30-s stimulus presentation (Fig. 2*B*, red and green lines). This dichotomy in the temporal profile and polarity of the responses is clearly evident when plotting the time to peak/trough as a function of the slope before peak/trough (Fig. 2*C*).

Effect of Light History on PFC Luxotonic Activation. Prior evidence demonstrated that antecedent light exposure can modulate subsequent brain activity and the emotional and cognitive processes mediated by the specific brain region (42–44). To control for possible effects of the immediately preceding stimulus on the encoding of the current light intensity, we focused on the three transitions in which light intensity (L) was stepped up from the single, lowest intensity (L1 → L2, L1 → L3, and L1 → L4). This analysis revealed that the PFC activation in response to the second stimulus in each light-intensity pair (L2, L3, and L4) developed slowly throughout the 30-s duration (Fig. 3, *Left* panels). Steady-state PFC activation, measured as the average response over the last 10 s of the 30-s stimulus period, monotonically decreased with increasing light intensity in all five identified PFC luxotonic regions (Fig. 3, second column from the left), namely, the right and left superior frontal gyrus (SFG; S1, S2, S4), right OFC (S3), and right ACC (S5). We also found similar effects for individual participants (*SI Appendix*, Fig. S4). In addition to the five prefrontal regions, the pineal body (S10) also encoded steady-state light intensity; activation in the pineal body was similarly monotonically suppressed with increasing light intensity (*SI Appendix*, Fig. S5*B*). In contrast, the time course of light activation along the thalamo-visuocortical pathway differed (Fig. 4*A*). In the visual cortex (S6), activation increased sharply several seconds after the light onset, and then gradually declined, though the

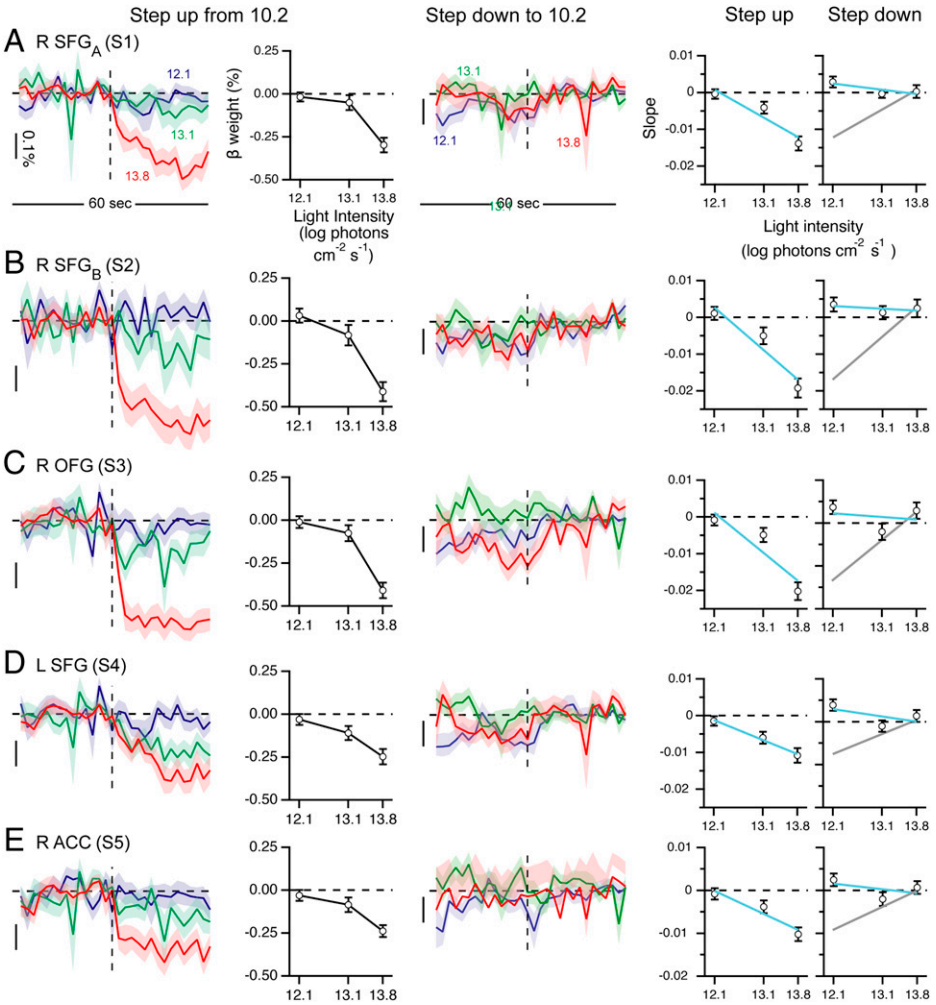

Fig. 3. Light suppresses steady-state prefrontal activity. (*A*–*E*, *Left*) BOLD Light-evoked responses (mean [line] ± SEM [shaded area]) step-up transitions: transitions in which light intensity was stepped up from the same, lowest, light intensity. Responses around individual transitions are depicted in different colors. Shaded gray areas represent the SE from the mean. Dashed vertical line marks the transition time. For example, the red curve in *A* represents stepping-up light intensity from the lowest level (L1, 10.2 log photons cm^{-2} s^{-1}) to the highest level (L4, 13.8 log photons cm^{-2} s^{-1}). Second column from left: Steady-state prefrontal activity monotonically decreased with increasing light intensity in all five identified prefrontal luxotonic regions. These are the left and right SFG (*A*, *B*, *D*), right OFC (*C*), and right ACC (*E*). Vertical bar representing 0.2 BOLD response in *A* applies to the amplitude of responses in *A*–*E*. Third column from left: BOLD light-evoked responses (mean ± SEM) to step-down transitions (transitions in which light intensity was stepped down from the same, highest, light intensity). Rightmost column: Slopes fitted to the three step-up and three step-down transitions. In the PFC in which activity decreased with light intensity, transitions to higher light intensities resulted in negative slopes, whereas transitions to lower light intensities resulted in positive slopes. With no effect of light history, the trend observed when moving across slope values for step-up transitions (cyan line) is expected to be the opposite of that of step-down transitions (gray line). The actual observed trend for step-down transitions is depicted (cyan line). The angular difference between the observed and expected trends for step-down transitions serves as a proxy for the strength of the effect of prior light history. Sample size, L1 → L2: n = 81, L1 → L3: n = 56, L1 → L4: n = 79, L2 → L1: n = 78, L3 → L1: n = 84, L4 → L1: n = 68.

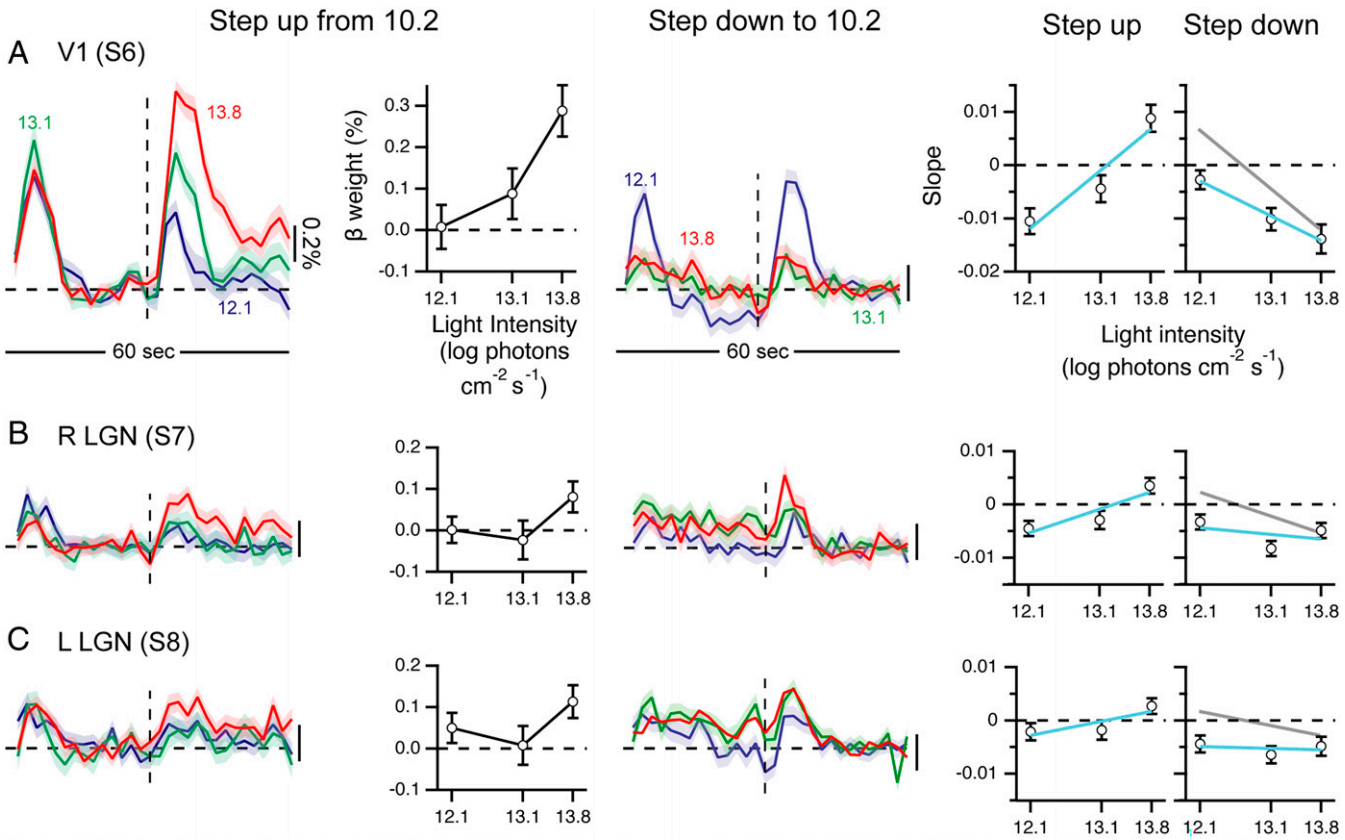

Fig. 4. Light enhances activity along the thalamo-visuocortical pathway. Conventions as in Fig. 3. (*A–C*, two leftmost columns). Steady-state activity (mean ± SEM) monotonically increased with increasing light intensity in all three luxotonic regions along the thalamo-visuocortical pathway. Vertical bar, representing 0.2 BOLD response in *A*, applies to all panels. In the visual cortex (*A*) and the right and left LGN (*B* and *C*), in which activity increased with light intensity, transitions to higher light intensities resulted in positive slopes, whereas transitions to lower light intensities resulted in zero or negative slopes. Sample size, L1 → L2: $n = 81$, L1 → L3: $n = 56$, L1 → L4: $n = 79$, L2 → L1: $n = 78$, L3 → L1: $n = 84$, L4 → L1: $n = 68$.

response did not return to baseline during the 30-s light stimulus of the highest light intensity (Fig. 4 *A*, *Left*). Similar trends were observed in the right (S7) and left (S8) LGN (Fig. 4 *B* and *C*, *Left*). While steady-state activation increased with light intensity in all three identified regions along the thalamo-visuocortical pathway (Fig. 4, second column from left), the magnitude of responses in the visual cortex was three times as large as that observed in the LGN. Activation in another luxotonic region, the cerebellar vermis (S9), also appeared to increase slightly with increasing light intensity (*SI Appendix*, Fig. S5*B*).

We next quantified the effect of prior light exposure on BOLD activation by plotting the three transitions in which light intensity was stepped down to the lowest intensity from higher levels: that is, L4 → L1, L3 → L1, and L2 → L1 (Fig. 3, third column from left). We then fit a straight line to the activation around a given transition and repeated this for the three step-up and the three step-down transitions. This procedure yielded three slope values for both the step-up transitions and the step-down transitions (Fig. 3, two rightmost columns). We reasoned that if brain activation was unaffected by prior light exposure, the trend observed when moving across slope values should be opposite, or close to, for the step-up and step-down transitions. Deviation from this expectation serves as a proxy for the strength of the effect of prior light exposure. While activation in all 10 identified luxotonic regions that exhibited a sustained response was affected by prior light exposure, the effect in the five prefrontal luxotonic regions (0.58 ± 0.15 BOLD response; mean ± SD) was significantly larger (permutation *t* test, $P < 0.001$) than in the other five regions not in the PFC (0.19 ± 0.05 BOLD response), and it was especially high in the right SFG and the right OFC (Fig. 3, *Right*, Fig. 4, *Right*, Fig. 5, and *SI Appendix*, Fig. S5, *Right*). These results demonstrate a strong effect of light history on PFC activation. Since ipRGCs, more so than conventional RGCs, can exhibit persistent responses following the light offset (45), this analysis raises the possibility that the observed PFC activation may be driven by ipRGCs.

Light-Induced Transient Activation in the Cerebral Cortex. In addition to the 10 luxotonic regions with a significant sustained component that we described above, we also identified 16 luxotonic regions (*SI Appendix*, Table S1) that showed activation with a significant transient component (see *Materials and Methods* for details on the regressor used for this analysis). These 16 regions correspond only to those that showed a light-intensity–dependent amplitude of the transient response rather than all regions showing a transient response (i.e., a contrast-dependent transient response). Therefore, the light-intensity–dependent transient activation detected in these 16 regions represented the remaining activation after the contrast-dependent transient response has been removed. Transient activation increased (orange) or decreased (blue) monotonically with light intensity (Fig. 6 and *SI Appendix*, Fig. S6). Light-intensity–dependent transient activation was detected bilaterally in the SFG (T2, T4), paracentral lobule (T7, T8), visual cortex (T10, T11), and lingual gyri (T12–T14). We observed right hemisphere-only transient activation in the superior medial gyrus (T1), frontal operculum (T5), precentral gyrus (T6), superior occipital gyrus (T15), and fusiform gyrus (T16). And, we found left hemisphere-only transient activation

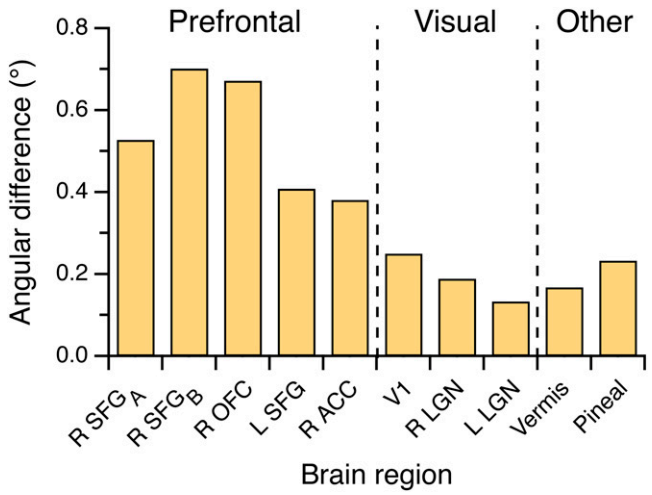

Fig. 5. High effect of prior light exposure on brain activity in the PFC. The magnitude of the effect of light history estimated as the angular difference between the observed and expected trends for step-down transitions. While prior light exposure affected all luxotonic regions, the effect on the PFC, and especially on the right SFG and right OFC was the largest.

in the middle OFC (T3), superior gyrus (T4), and intraparietal sulcus (IPS, T9).

We next assessed whether the 16 luxotonic regions that showed a transient component formed independent or dependent networks by assessing their functional connectivity (*SI Appendix*, Fig. S7). BOLD time-series in the frontal cortex showed two distinct activation sets, one in the PFC (set *a*) and another in more posterior regions including motor areas (set *b*). Time series in the parietal lobe (set *c*) positively correlated with those in the prefrontal regions but negatively correlated with all other regions. Time series in the occipital and temporal lobes correlated with one another (set *d*) and with the frontal regions (set *e*).

Next, just as we did for luxotonic regions in which activation exhibited a sustained component (Figs. 3 and 4 and *SI Appendix*, Fig. S5), we assessed the light-intensity–encoding capability of the 16 identified luxotonic regions with a transient component while controlling for prior light exposure; that is, we examined the three transitions in which light intensity was stepped up from the lowest intensity (*SI Appendix*, Fig. S8). Light-intensity–dependent activation level typically changed abruptly upon light onset, then declined, although in several regions the activation persisted throughout the 30-s duration of the stimulus. Activation in the SFG and the middle OFC (regions T1 to T4) decreased sharply following light onset, remained relatively low throughout the 30-s duration of the stimulus, and typically decreased monotonically with increasing light intensity. Activation in the 12 remaining identified regions increased upon light onset and then gradually tapered off. In some regions (e.g., visual cortex, T11) activation did not return to baseline during the 30-s light stimulus.

Luxotonic Regions Exhibiting Sustained and Transient Activation Co-Occur Along a Streak in the Occipital Lobe. Finally, we examined the overlap luxotonic regions having a significant sustained component and those having a significant transient component. We found little overlap except for one nearly contiguous strip running along the parieto-occipital sulcus and the dorsal cuneus (Fig. 7), indicating near complete anatomical segregation between brain regions showing sustained or transient responses to steady-state light stimuli. Sustained activation comprised 3,678 voxels and transient activation comprised 1,735 voxels, for a total of 5,413 voxels. Of these, 350 voxels showed overlap for transient and sustained activation, corresponding to ∼6% of the combined activation.

Discussion

While luxotonic activation in the early human visual cortex has been previously documented (37–39), we now report luxotonic-related activation in the human PFC, precentral gyrus, paracentral lobule, frontal operculum, intraparietal sulcus, LGN, fusiform and lingual gyrus, pineal body, and portions of the cerebellum. Therefore, we now demonstrate that light intensity alters the physiology of diverse human brain regions that collectively contribute to motor control, cognition, emotion, and reward; thus, well beyond those subsumed by the classic form vision pathways. We identified 26 human brain regions in which activation either monotonically decreased or increased with light intensity, with 10 regions showing significant sustained activation and 16 other regions exhibiting a significant transient activation pattern. All the regions with a monotonically decreasing pattern in response to increasing light intensity had responses that persisted until the termination of the light stimulus.

Acute Effect of Light on Steady-State PFC Activation. Prior observations have suggested light-evoked modulation of several prefrontal regions. For example, blue light exposure (as opposed to green or orange), concurrently with an auditory working memory task, increased activation in the left middle frontal gyrus (8, 9) and decreased ACC activation (9). Furthermore, blue light (as opposed to amber) decreased ACC activation following an emotional anticipation task (46). However, our observations uniquely demonstrate wide-ranging effects of light on PFC physiology, which varied monotonically with light intensity. We did not, however, examine the influence of ambient illumination on activation related to the auditory discrimination task, though neither reaction time to the tones nor discrimination accuracy differed across the illumination intensities. We identified five regions having a sustained-activation pattern in the PFC: right and left SFG, right OFC, and right ACC. These regions have clear involvement in cognitive and emotional processes. For example, the left SFG is involved in self-awareness (47) and spatial working memory (48). In the right hemisphere, this region contributes to the control of impulsive responses or action inhibition (49). The ACC contributes to social cognition, attention allocation, motivation, decision making, learning, cost–benefit calculation, impulse control, and emotion (50, 51). Additionally, the OFC is involved in learning and reversing associations between taste, smell, somatosensory, and visual information, and in controlling reward-related and punishment-related behaviors. Thus, the OFC participates in shaping motivational, emotional, and social behaviors (52, 53). Our results demonstrate that activation in all five identified prefrontal luxotonic regions decreased with light intensity and offer a possible functional link between prefrontal light processing and several cognitive and affective phenomena previously reported to be affected by light intensity.

Chronic Effect of Light on Prefrontal Activation. In addition to the acute effect of light on neural activation, light can also chronically affect neural activation. We found a pronounced effect of light exposure on subsequent activation in the five prefrontal luxotonic regions, particularly in the right SFG and the right OFC. Activation in those regions, which comprise portions of the mPFC, was suppressed during and subsequent to light exposure. Such chronic suppression of brain activation by light has

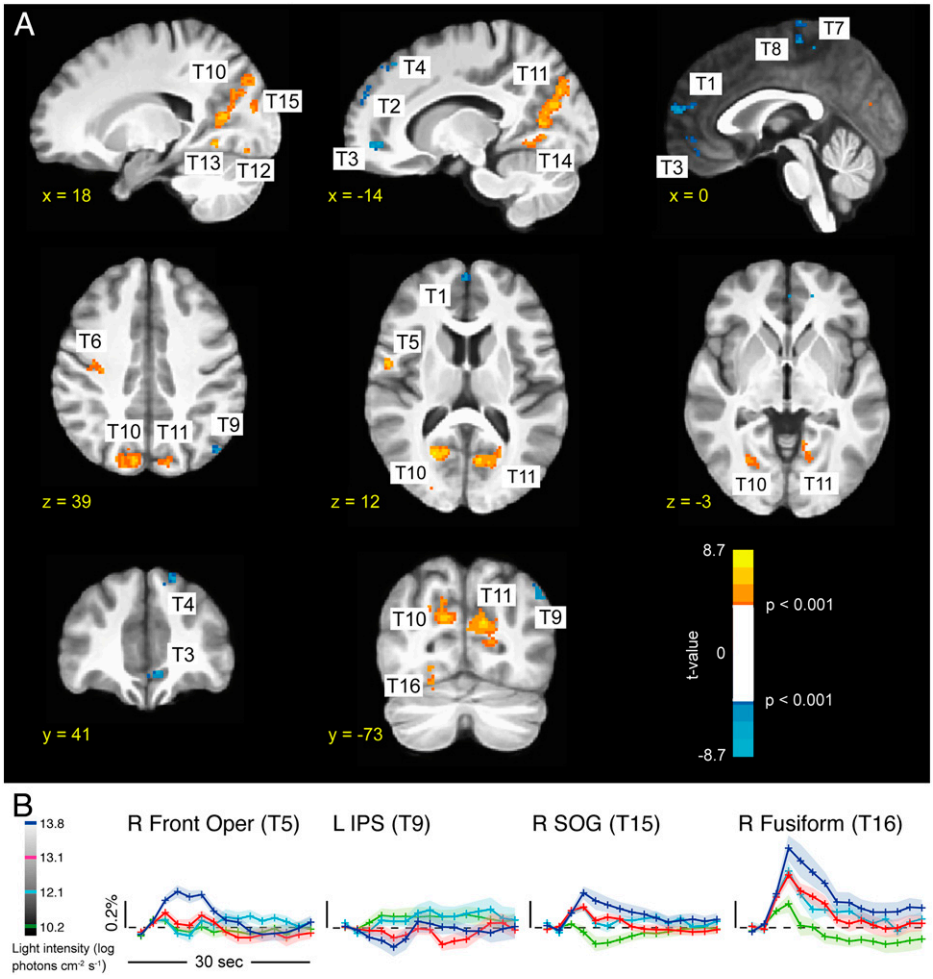

Fig. 6. Cortical luxotonic regions that show a significant transient component. (*A*) The 16 identified luxotonic regions are color-coded based on the contrast for monotonic increases or decreases as a function of light intensity. The MNI coordinates of presented slices are indicated in yellow. Color scale corresponds to *t* value: warm colors (positive *t*), light-evoked responses increase with light intensity; cool colors (negative *t*), light-evoked responses decrease with light intensity. Color bar, *t* values ranges ±8.7, and images are thresholded at $P < 0.001$, $t_{19} = 3.621$ (white horizontal lines). Anatomical underlay represents the mean of all 20 participants following spatial alignment. Regions: T1, right superior medial gyrus (R SMG); T2, R SFG; T3, left middle orbital gyrus (L mOFG); T4, L SFG; T5, R frontal operculum; T6, R precentral gyrus; T7, R paracentral lobule; T8, L paracentral lobule; T9, L IPS; T10, R V1; T11, L V1; T12, right lingual gyrus A (R $LingG_A$); T13, R $LingG_B$; T14, L. LingG; T15, right superior occipital gyrus (R SOG); T16, right fusiform gyrus (R FusiG). (*B*) BOLD responses (mean ± SEM) for T5, T9, T15, and T16 over the 30-s light stimulus, for four light intensities. Data for all the luxotonic regions are shown in *SI Appendix*, Fig. S4.

not been previously reported in these regions, but chronic enhancement of neural activation by light has been reported in other brain regions. For example, a single 30-min exposure to blue light as opposed to amber light (expected to activate the blue-sensitive melanopsin photopigment of ipRGCs) has been shown to improve working memory task performance and increase activation in the dorsolateral PFC (dlPFC) and ventrolateral PFC (vlPFC) over the subsequent 40-min period (42). Another study, using a shorter light exposure (21 min), reported increased activation over the subsequent 8-min period in the hippocampus, right ACC, left precuneus, and right IPS (43). Our demonstration of a chronic effect of light on PFC activation complements previous reports and may constitute the substrate for the previously reported effects of light on decision making, social behavior, working memory, and mood (2, 42, 44, 54, 55).

Origin of Prefrontal Luxotonic Responses. The slowly evolving and persistent responses we observed in the human PFC have similarity to ipRGCs responses. ipRGCs responses in humans (25), as well as in the mouse (12–14, 56), persist throughout the duration of the stimulus and even after light offset, with the poststimulus response duration increasing with light intensity. Thus, the similarity in light-evoked activity in ipRGCs and the human PFC may suggest a contribution of ipRGCs' light responses to PFC activation. While ipRGCs also receive synaptic input from rod and cone photoreceptors, their melanopsin pigment is especially sensitive to blue light wavelengths (15), which appear to shape PFC-mediated functions in humans. For example, blue-enriched white light occurring in the evening (as opposed to white light), either in the environment or emitted by a computer screen, improves cognitive performance, alertness, and concentration (57, 58). Additionally, improvement in cognitive performance under blue-enriched lighting occurs during the daylight hours (59). At least some of these cognitive functions have been shown to depend on ipRGCs, thus linking specific frontal functions to a unique ipRGCs sensitivity. For example, in blind individuals who lack rod and cone photoreceptors but retain ipRGCs, blue light exposure during an auditory task increases activation in the mPFC and vlPFC (60), supporting the notion that the light-evoked modulation we observed in the PFC had contributions from ipRGCs. Together, these reports suggest that blue light-sensitivity drives alterations in cognition and frontal brain activation, and it occurs specifically by activity of ipRGCs.

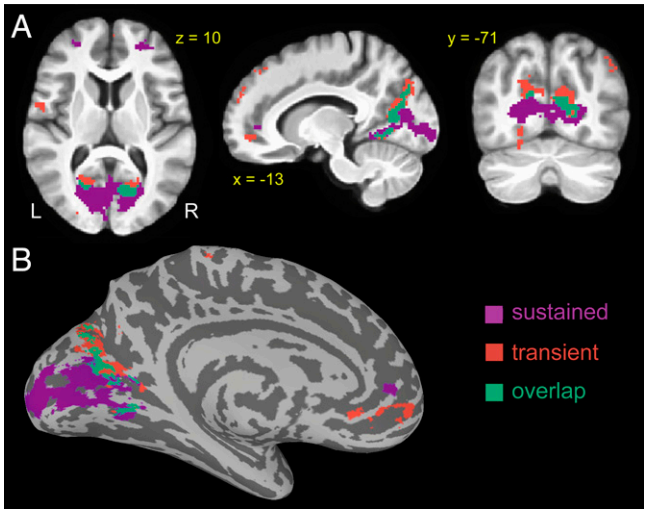

Fig. 7. Sustained and transient response regions along the parieto-occipital sulcus. (*A*) Horizontal, mid sagittal, and coronal sections showing the overlap between luxotonic regions in which activity showed both significant sustained and transient components. Sustained and transient regions are marked in purple and in red, respectively, and overlapping areas are marked in green. The MNI coordinates of presented slices are indicated in yellow. (*B*) Same data presented on an inflated brain model.

The rapidly developing and decaying responses we observed in V1 and the LGN resemble responses of conventional RGCs (non-ipRGCs). Conventional RGCs do not express melanopsin; they respond to alterations in light intensity only briefly, and their maintained firing rates do not correlate with photon flux (61, 62). Conventional RGCs encode temporal and spatial contrast, and support the object detection and recognition, color, depth, and motion (63, 64), especially via signals routed through the thalamus to the primary and extrastriate visual cortices. Interestingly, the luxotonic activity we observed in V1 and the LGN did not return to baseline by stimulus termination, suggesting, but not proving, a modest ipRGCs' contribution to this activation pattern. Indeed, melanopsin, the blue-sensitive pigment of ipRGCs, contributes to light-evoked response in the human V1 (65); and, while the majority of input to the mouse dLGN, which routes information to visual cortices, arrives from conventional RGCs, at least some ipRGC types do project to the dLGN (66). Therefore, the light-evoked activation we observed in the visual cortex and LGN likely represents the integration of signals from both ipRGCs and conventional RGCs.

The frontal regions with light-intensity–dependent activation in humans did not have a clear correspondence to frontal cortical regions in mice, which based on anatomical data also likely exhibit light-intensity sensitivity, although new experiments would have to demonstrate such sensitivity. In mice, the thalamic PHb projects to the infralimbic and prelimbic cortices (20), raising the possibility that luxotonic neural input is transmitted from the PHb to those limbic cortices. We did not find light-intensity–dependent activation in the infralimbic and prelimbic cortices of humans. However, our relatively conservative cluster size criterion (27 voxels), the relatively limited size of the human infralimbic and prelimbic cortices, or differences in homologous pathways between humans and mice could readily explain this discrepancy. While it is currently unknown whether the human PFC is part of a pathway homologous to the retinal-thalamic-frontocortical pathway discovered in mice, the persistence and luxotonic nature of light-evoked responses in the human PFC strongly suggests that it receives input from ipRGCs, similar to the pathway in mice (20). Knowing the spectral sensitivity of melanopsin in humans (479 nm) (67), unlike the present study that used a white-light stimulus, future studies may utilize discrete monochromatic stimuli to reveal whether the light-intensity–dependent activation we observed here is greatest at the peak spectral sensitivity of melanopsin. Moreover, mouse PHb neurons that receive ipRGCs input, along with PHb neurons that project to the NAc, are mainly GABAergic (23). If a subset of mPFC-projecting PHb neurons is also GABAergic, this feature would raise the possibility that the mouse PHb transmits inhibitory drive to the PFC. If discovered in humans, PHb-to-mPFC inhibitory input may explain our observation that light exposure suppressed prefrontal activation.

Human PFC and Mood Regulation. The PFC is commonly divided, based on connectivity and functional specialization, into the dlPFC and ventromedial PFC (vmPFC) (35, 68). Resting-state brain activation (26, 28) and glucose metabolic rates (28, 29) in the vmPFC, including the OFC, are higher in depressed people, whereas the metabolic rate in dlPFC of depressed people appears low (28, 30). Recovery from depression and antidepressants affect the vmPFC and dlPFC in an opposite manner. Specifically, antidepressants and the accompanying recovery from depression is associated with decreased vmPFC activation but increased dlPFC activation (31, 32). Here, we found light-evoked suppression of the PFC, including in the OFC. Therefore, similar to antidepressants, light appears to reduce activation in these regions.

Effect of Light on the Cerebellum and Pineal Body. We identified a luxotonic region in the uvula that constitutes a large portion of the cerebellar inferior vermis. Activation in this region was enhanced with light exposure. The uvula is activated during optokinetic eye movements, and this activation depends on the speed and direction of eye movements (69). Interestingly, oculomotor performance has been shown to depend on light intensity, resulting in eye movements of greater accuracy in the light compared to darkness (70), suggesting a possible functional role for the uvula's light-intensity–dependent activation in oculomotor responses.

The melatonin-producing pineal gland modulates sleep and circadian and seasonal rhythms (71). It receives indirect photic input from ipRGCs (via the paraventricular hypothalamic nucleus, intermediolateral nucleus of the spinal cord, and superior cervical ganglion) (72). Our observation that light exposure suppresses pineal BOLD activation in a light-intensity–dependent manner is consistent with the known suppression of melatonin production in response to light (73). This light-induced melatonin suppression is retained following severe degeneration of rods and cones, in both humans (74) and mice (75). Its spectral tuning is strikingly similar to that of melanopsin, rather than to that of rods or cones (76), and is a common assay for the integrity of the nonimage-forming visual system. The similar form of the pineal and prefrontal light-evoked responses, and its divergence from light responses in the visual cortex and LGN, is yet another plausible indicator for ipRGCs contribution to the observed suppression of prefrontal activation by light.

An Overlap Between Luxotonic Regions in Which Activation Showed Significant Sustained and Transient Components. While this study focused on how light exposure affects steady-state brain activation, we also identified 16 brain regions exhibiting a significant transient component that varied monotonically with light intensity. These regions are merely those in which

light-evoked transient activity has been detected. Instead, activation in these regions varied monotonically with light intensity after removing any contrast-dependent responses associated with stepping light intensity, either down or up. These regions included the right precentral gyrus (primary motor cortex, T6), which together with the paracentral lobule (T7, T8) and other structures participate in planning, regulating, and performing voluntary movements (77). Indeed, light clearly has a role in shaping locomotion-related neuronal activity recorded from the motor cortex (78). The frontal operculum (T5) is a critical node in a network controlling activation in other brain areas with roles in a wide array of cognitive tasks (79–81). The fusiform gyrus (T16) appears critical for visual categorization and high-level visual processing, including the processing of information related to faces and bodies (82–85). The lingual gyrus contributes to visual and semantic memory and word processing (86–88). The IPS region (T9) integrates visual and sensorimotor signals for guiding and controlling spatial action (89, 90), and contributes to object manipulation and grasping movements (91), attention processes, and eye movement control (92). Finding luxotonic regions in these cortical areas raises the possibility that light likely modulates processing in some of them, thereby possibly influencing a wide array of sensory, motor, emotional, and cognitive functions. Further study into the effect of light exposure on those brain regions and the functions they mediate would shed light on these questions. We have found that sustained and transient responsive regions were almost completely segregated, except for one nearly contiguous strip running along the parieto-occipital sulcus and the dorsal cuneus, which is in a position to modify information transferred from the primary visual cortex to extrastriate cortices (93).

Horiguchi et al. (94) extracted the relative contributions of transient and sustained neural channels that appear to be interleaved at the scale of a typical 2-mm isotropic fMRI voxel. The central visual field representation was reported to include a significant sustained response, with the amplitude of the sustained channel signal declining with eccentricity. In the present study, we utilized transient and sustained temporal channels similar to those previously used, but only after removing the contrast-dependent response driven by transitions between light intensities. This was achieved by subtracting from the BOLD response a third channel that accounted for the transitions between light intensities.

The activation pattern we observed in V1 is consistent with previous studies that reported the effect of long-duration diffused light stimuli in V1 (39, 94, 95). Our results also demonstrate the contribution of sustained and transient components to activation in the visual cortex (*SI Appendix*, Fig. S8). However, because we removed the contrast-dependent component from the BOLD response, in our hands, the extent across which the transient component dominated was restricted to smaller areas than reported previously. Indeed, without removing the contrast-dependent response, the activation pattern in the visual cortex better resembled previously reported activation (*SI Appendix*, Fig. S9). Future work could explore more sophisticated models to account for the contribution of the sustained and transient response activation components. For example, the model used by Stigliani et al. (96) that considers prior knowledge on the neural response might prove useful to disentangle the two seemingly opposing effects.

See *SI Appendix* for a description of alternative sources of time-locked increases in brain activation.

Materials and Methods

Twenty healthy female and male participants provided written informed consent and received modest monetary compensation. This study was approved by the Brown University Institutional Review Board. We used BOLD fMRI to explore whole-brain activation patterns in response to full-field diffused-light stimuli at four intensities. To ensure alertness during the scan session, participants performed an auditory discrimination task. Data were warped to Montreal Neurological Institute (MNI) space for anatomical alignment, slice time- and motion-corrected, spatially smoothed, and normalized. Independent regressors were used to reveal brain regions having sustained or transient activation that varied monotonically with light intensity, while accounting for the contrast-dependent response related to the relative change in light intensity from one stimulus to the next. See *SI Appendix, Supplementary Materials and Methods* for further description.

Data Availability. The raw data and source code required to reproduce all analyses and figures in this paper are deposited in FigShare (https://doi.org/10.6084/m9.figshare.c.6054941.v1) (97). We have deposited the raw data at OpenNeuro (https://openneuro.org), including the magnetic resonance images, identifying information about stimulus light intensity, individual participant coding, and the time and outcome of the auditory task, and using the following accession number: ds004065 (98).

ACKNOWLEDGMENTS. We thank Rebecca Waugh, a former research assistant at the Brown University MRI Research Facility, for her work on data collection and initial analyses, and Eli Shmueli for valuable comments on the manuscript. This project was supported by grants from the National Institute of Psychobiology of Israel and the Banting Postdoctoral Fellowship of Canada (S.S.); NIH Grant R01 EY12793 and an Alcon Research Institute award (to D.M.B.); and NIH Grants P20GM103645 and S10OD025181 and the Division of Biology and Medicine, Brown University (to J.N.S.).

1. L. K. Fonken, E. Kitsmiller, L. Smale, R. J. Nelson, Dim nighttime light impairs cognition and provokes depressive-like responses in a diurnal rodent. *J. Biol. Rhythms* **27**, 319–327 (2012).
2. T. A. Bedrosian, Z. M. Weil, R. J. Nelson, Chronic dim light at night provokes reversible depression-like phenotype: Possible role for TNF. *Mol. Psychiatry* **18**, 930–936 (2013).
3. M. M. Gonzalez, G. Aston-Jones, Light deprivation damages monoamine neurons and produces a depressive behavioral phenotype in rats. *Proc. Natl. Acad. Sci. U.S.A.* **105**, 4898–4903 (2008).
4. R. W. Lam *et al.*, Efficacy of bright light treatment, fluoxetine, and the combination in patients with nonseasonal major depressive disorder: A randomized clinical trial. *JAMA Psychiatry* **73**, 56–63 (2016).
5. T. M. Penders *et al.*, Bright light therapy as augmentation of pharmacotherapy for treatment of depression: A systematic review and meta-analysis. *Prim. Care Companion CNS Disord.* **18**, 10.4088/PCC.15r01906 (2016).
6. D. K. Sit *et al.*, Adjunctive bright light therapy for bipolar depression: A randomized double-blind placebo-controlled trial. *Am. J. Psychiatry* **175**, 131–139 (2018).
7. T. A. Bedrosian, R. J. Nelson, Timing of light exposure affects mood and brain circuits. *Transl. Psychiatry* **7**, e1017 (2017).
8. G. Vandewalle *et al.*, Wavelength-dependent modulation of brain responses to a working memory task by daytime light exposure. *Cereb. Cortex* **17**, 2788–2795 (2007).
9. V. Daneault *et al.*, Plasticity in the sensitivity to light in aging: Decreased non-visual impact of light on cognitive brain activity in older individuals but no impact of lens replacement. *Front. Physiol.* **9**, 1557 (2018).
10. A. J. Xu, A. A. Labroo, Incandescent affect: Turning on the hot emotional system with bright light. *J. Consum. Psychol.* **24**, 207–216 (2014).
11. V. Kretschmer, K. H. Schmidt, B. Griefahn, Bright light effects on working memory, sustained attention and concentration of elderly night shift workers. *Light. Res. Technol.* **44**, 316–333 (2012).
12. K. Y. Wong, A retinal ganglion cell that can signal irradiance continuously for 10 hours. *J. Neurosci.* **32**, 11478–11485 (2012).
13. T. M. Schmidt, P. Kofuji, Functional and morphological differences among intrinsically photosensitive retinal ganglion cells. *J. Neurosci.* **29**, 476–482 (2009).
14. S. Sabbah *et al.*, Intrinsically photosensitive retinal ganglion cells evade temporal filtering to encode environmental light intensity bioRxiv [Preprint] (2022). https://doi.org/10.1101/2022.04.09.487733 (Accessed 1 July 2022).
15. D. M. Berson, F. A. Dunn, M. Takao, Phototransduction by retinal ganglion cells that set the circadian clock. *Science* **295**, 1070–1073 (2002).
16. J. L. Ecker *et al.*, Melanopsin-expressing retinal ganglion-cell photoreceptors: Cellular diversity and role in pattern vision. *Neuron* **67**, 49–60 (2010).
17. S. K. Chen, T. C. Badea, S. Hattar, Photoentrainment and pupillary light reflex are mediated by distinct populations of ipRGCs. *Nature* **476**, 92–95 (2011).
18. T. A. LeGates, D. C. Fernandez, S. Hattar, Light as a central modulator of circadian rhythms, sleep and affect. *Nat. Rev. Neurosci.* **15**, 443–454 (2014).
19. T. A. LeGates *et al.*, Aberrant light directly impairs mood and learning through melanopsin-expressing neurons. *Nature* **491**, 594–598 (2012).
20. D. C. Fernandez *et al.*, Light affects mood and learning through distinct retina-brain pathways. *Cell* **175**, 71–84.e18 (2018).
21. E. A. Murray, S. P. Wise, W. C. Drevets, Localization of dysfunction in major depressive disorder: Prefrontal cortex and amygdala. *Biol. Psychiatry* **69**, e43–e54 (2011).

22. W. C. Drevets, J. L. Price, M. L. Furey, Brain structural and functional abnormalities in mood disorders: Implications for neurocircuitry models of depression. *Brain Struct. Funct.* **213**, 93–118 (2008).
23. K. An *et al.*, A circadian rhythm-gated subcortical pathway for nighttime-light-induced depressive-like behaviors in mice. *Nat. Neurosci.* **23**, 869–880 (2020).
24. A. M. Graybiel, S. T. Grafton, The striatum: Where skills and habits meet. *Cold Spring Harb. Perspect. Biol.* **7**, a021691 (2015).
25. L. S. Mure, F. Vinberg, A. Hanneken, S. Panda, Functional diversity of human intrinsically photosensitive retinal ganglion cells. *Science* **366**, 1251–1255 (2019).
26. W. C. Drevets *et al.*, A functional anatomical study of unipolar depression. *J. Neurosci.* **12**, 3628–3641 (1992).
27. M. D. Greicius *et al.*, Resting-state functional connectivity in major depression: Abnormally increased contributions from subgenual cingulate cortex and thalamus. *Biol. Psychiatry* **62**, 429–437 (2007).
28. F. Biver *et al.*, Frontal and parietal metabolic disturbances in unipolar depression. *Biol. Psychiatry* **36**, 381–388 (1994).
29. W. C. Drevets, W. Bogers, M. E. Raichle, Functional anatomical correlates of antidepressant drug treatment assessed using PET measures of regional glucose metabolism. *Eur. Neuropsychopharmacol.* **12**, 527–544 (2002).
30. L. R. Baxter Jr. *et al.*, Reduction of prefrontal cortex glucose metabolism common to three types of depression. *Arch. Gen. Psychiatry* **46**, 243–250 (1989).
31. A. L. Brody *et al.*, Brain metabolic changes associated with symptom factor improvement in major depressive disorder. *Biol. Psychiatry* **50**, 171–178 (2001).
32. H. S. Mayberg *et al.*, Reciprocal limbic-cortical function and negative mood: Converging PET findings in depression and normal sadness. *Am. J. Psychiatry* **156**, 675–682 (1999).
33. M. Li, H. Xu, S. Lu, Neural basis of depression related to a dominant right hemisphere: A resting-state fMRI study. *Behav. Neurol.* **2018**, 5024520 (2018).
34. S. M. Palmer, S. G. Crewther, L. M. Carey, S. P. Team; START Project Team, A meta-analysis of changes in brain activity in clinical depression. *Front. Hum. Neurosci.* **8**, 1045 (2015).
35. M. Koenigs, J. Grafman, The functional neuroanatomy of depression: Distinct roles for ventromedial and dorsolateral prefrontal cortex. *Behav. Brain Res.* **201**, 239–243 (2009).
36. M. Liotti, D. M. Tucker, Right hemisphere sensitivity to arousal and depression. *Brain Cogn.* **18**, 138–151 (1992).
37. L. N. Vinke, S. Ling, Luminance potentiates human visuocortical responses. *J. Neurophysiol.* **123**, 473–483 (2020).
38. H. Boyaci, F. Fang, S. O. Murray, D. Kersten, Responses to lightness variations in early human visual cortex. *Curr. Biol.* **17**, 989–993 (2007).
39. J.-D. Haynes, R. B. Lotto, G. Rees, Responses of human visual cortex to uniform surfaces. *Proc. Natl. Acad. Sci. U.S.A.* **101**, 4286–4291 (2004).
40. F. W. Cornelissen, A. R. Wade, T. Vladusich, R. F. Dougherty, B. A. Wandell, No functional magnetic resonance imaging evidence for brightness and color filling-in in early human visual cortex. *J. Neurosci.* **26**, 3634–3641 (2006).
41. J. T. Hull, C. A. Czeisler, S. W. Lockley, Suppression of melatonin secretion in totally visually blind people by ocular exposure to white light: Clinical characteristics. *Ophthalmology* **125**, 1160–1171 (2018).
42. A. Alkozei *et al.*, Exposure to blue light increases subsequent functional activation of the prefrontal cortex during performance of a working memory task. *Sleep (Basel)* **39**, 1671–1680 (2016).
43. G. Vandewalle *et al.*, Daytime light exposure dynamically enhances brain responses. *Curr. Biol.* **16**, 1616–1621 (2006).
44. L. L. Shan *et al.*, Light exposure before learning improves memory consolidation at night. *Sci. Rep.* **5**, 15578 (2015).
45. J. J. Pang, F. Gao, S. M. Wu, Light-evoked excitatory and inhibitory synaptic inputs to ON and OFF alpha ganglion cells in the mouse retina. *J. Neurosci.* **23**, 6063–6073 (2003).
46. A. Alkozei, R. Smith, W. D. S. Killgore, Exposure to blue wavelength light modulates anterior cingulate cortex activation in response to 'uncertain' versus 'certain' anticipation of positive stimuli. *Neurosci. Lett.* **616**, 5–10 (2016).
47. I. I. Goldberg, M. Harel, R. Malach, When the brain loses its self: Prefrontal inactivation during sensorimotor processing. *Neuron* **50**, 329–339 (2006).
48. S. M. Courtney, L. Petit, J. M. Maisog, L. G. Ungerleider, J. V. Haxby, An area specialized for spatial working memory in human frontal cortex. *Science* **279**, 1347–1351 (1998).
49. S. Hu, J. S. Ide, S. Zhang, C. R. Li, The right superior frontal gyrus and individual variation in proactive control of impulsive response. *J. Neurosci.* **36**, 12688–12696 (2016).
50. A. J. Shackman *et al.*, The integration of negative affect, pain and cognitive control in the cingulate cortex. *Nat. Rev. Neurosci.* **12**, 154–167 (2011).
51. K. R. Ridderinkhof, M. Ullsperger, E. A. Crone, S. Nieuwenhuis, The role of the medial frontal cortex in cognitive control. *Science* **306**, 443–447 (2004).
52. E. T. Rolls, The functions of the orbitofrontal cortex. *Brain Cogn.* **55**, 11–29 (2004).
53. E. T. Rolls, W. Cheng, J. Feng, The orbitofrontal cortex: Reward, emotion and depression. *Brain Commun.* **2**, a196 (2020).
54. N. Wessolowski, H. Koenig, M. Schulte-Markwort, C. Barkmann, The effect of variable light on the fidgetiness and social behavior of pupils in school. *J. Environ. Psychol.* **39**, 101–108 (2014).
55. I. Knez, Effects of colour of light nonvisual psychological processes. *J. Environ. Psychol.* **21**, 201–208 (2001).
56. M. E. Estevez *et al.*, Form and function of the M4 cell, an intrinsically photosensitive retinal ganglion cell type contributing to geniculocortical vision. *J. Neurosci.* **32**, 13608–13620 (2012).
57. A. U. Viola, L. M. James, L. J. Schlangen, D. J. Dijk, Blue-enriched white light in the workplace improves self-reported alertness, performance and sleep quality. *Scand. J. Work Environ. Health* **34**, 297–306 (2008).
58. C. Cajochen *et al.*, Evening exposure to a light-emitting diodes (LED)-backlit computer screen affects circadian physiology and cognitive performance. *J. Appl. Physiol. (1985)* **110**, 1432–1438 (2011).
59. S. Lehrl *et al.*, Blue light improves cognitive performance. *J. Neural Transm. (Vienna)* **114**, 457–460 (2007).
60. G. Vandewalle *et al.*, Blue light stimulates cognitive brain activity in visually blind individuals. *J. Cogn. Neurosci.* **25**, 2072–2085 (2013).
61. S. Sabbah, D. Berg, C. Papendorp, K. L. Briggman, D. M. Berson, A Cre mouse line for probing irradiance- and direction-encoding retinal networks. *eNeuro* **4**, ENEURO.0065-17.2017 (2017).
62. T. Baden *et al.*, The functional diversity of retinal ganglion cells in the mouse. *Nature* **529**, 345–350 (2016).
63. J. R. Sanes, R. H. Masland, The types of retinal ganglion cells: Current status and implications for neuronal classification. *Annu. Rev. Neurosci.* **38**, 221–246 (2015).
64. W. Wei, A. M. Hamby, K. Zhou, M. B. Feller, Development of asymmetric inhibition underlying direction selectivity in the retina. *Nature* **469**, 402–406 (2011).
65. M. Spitschan *et al.*, The human visual cortex response to melanopsin-directed stimulation is accompanied by a distinct perceptual experience. *Proc. Natl. Acad. Sci. U.S.A.* **114**, 12291–12296 (2017).
66. J. Hannibal *et al.*, Central projections of intrinsically photosensitive retinal ganglion cells in the macaque monkey. *J. Comp. Neurol.* **522**, 2231–2248 (2014).
67. H. J. Bailes, R. J. Lucas, Human melanopsin forms a pigment maximally sensitive to blue light (λmax $\approx$ 479 nm) supporting activation of G(q/11) and G(i/o) signalling cascades. *Proc. Biol. Sci.* **280**, 20122987 (2013).
68. M. L. Kringelbach, E. T. Rolls, The functional neuroanatomy of the human orbitofrontal cortex: Evidence from neuroimaging and neuropsychology. *Prog. Neurobiol.* **72**, 341–372 (2004).
69. R. M. Ruehl, C. Hinkel, T. Bauermann, P. Z. Eulenburg, Delineating function and connectivity of optokinetic hubs in the cerebellum and the brainstem. *Brain Struct. Funct.* **222**, 4163–4185 (2017).
70. L. Goffart, J. Quinet, F. Chavane, G. S. Masson, Influence of background illumination on fixation and visually guided saccades in the rhesus monkey. *Vision Res.* **46**, 149–162 (2006).
71. M. M. Macchi, J. N. Bruce, Human pineal physiology and functional significance of melatonin. *Front. Neuroendocrinol.* **25**, 177–195 (2004).
72. J. Borjigin, L. S. Zhang, A. A. Calinescu, Circadian regulation of pineal gland rhythmicity. *Mol. Cell. Endocrinol.* **349**, 13–19 (2012).
73. A. J. Lewy, T. A. Wehr, F. K. Goodwin, D. A. Newsome, S. P. Markey, Light suppresses melatonin secretion in humans. *Science* **210**, 1267–1269 (1980).
74. C. A. Czeisler *et al.*, Suppression of melatonin secretion in some blind patients by exposure to bright light. *N. Engl. J. Med.* **332**, 6–11 (1995).
75. R. J. Lucas, M. S. Freedman, M. Muñoz, J. M. Garcia-Fernández, R. G. Foster, Regulation of the mammalian pineal by non-rod, non-cone, ocular photoreceptors. *Science* **284**, 505–507 (1999).
76. G. C. Brainard *et al.*, Action spectrum for melatonin regulation in humans: Evidence for a novel circadian photoreceptor. *J. Neurosci.* **21**, 6405–6412 (2001).
77. S. H. Lim *et al.*, Functional anatomy of the human supplementary sensorimotor area: Results of extraoperative electrical stimulation. *Electroencephalogr. Clin. Neurophysiol.* **91**, 179–193 (1994).
78. M. C. Armer, W. U. Nilaweera, T. J. Rivers, N. M. Dasgupta, I. N. Beloozerova, Effect of light on the activity of motor cortex neurons during locomotion. *Behav. Brain Res.* **250**, 238–250 (2013).
79. N. U. Dosenbach *et al.*, A core system for the implementation of task sets. *Neuron* **50**, 799–812 (2006).
80. D. A. Fair *et al.*, Development of distinct control networks through segregation and integration. *Proc. Natl. Acad. Sci. U.S.A.* **104**, 13507–13512 (2007).
81. T. Eichele *et al.*, Prediction of human errors by maladaptive changes in event-related brain networks. *Proc. Natl. Acad. Sci. U.S.A.* **105**, 6173–6178 (2008).
82. M. V. Peelen, P. E. Downing, Selectivity for the human body in the fusiform gyrus. *J. Neurophysiol.* **93**, 603–608 (2005).
83. K. S. Weiner, K. Grill-Spector, The improbable simplicity of the fusiform face area. *Trends Cogn. Sci.* **16**, 251–254 (2012).
84. L. R. Arcurio, J. M. Gold, T. W. James, The response of face-selective cortex with single face parts and part combinations. *Neuropsychologia* **50**, 2454–2459 (2012).
85. J. Liu, A. Harris, N. Kanwisher, Perception of face parts and face configurations: An FMRI study. *J. Cogn. Neurosci.* **22**, 203–211 (2010).
86. J. Bogousslavsky, J. Miklossy, J. P. Deruaz, G. Assal, F. Regli, Lingual and fusiform gyri in visual processing: A clinico-pathologic study of superior altitudinal hemianopia. *J. Neurol. Neurosurg. Psychiatry* **50**, 607–614 (1987).
87. S. A. Kozlovskiy *et al.*, Activation of left lingual gyrus related to working memory for schematic faces. *Int. J. Psychophysiol.* **94**, 241 (2014).
88. A. Mechelli, G. W. Humphreys, K. Mayall, A. Olson, C. J. Price, Differential effects of word length and visual contrast in the fusiform and lingual gyri during reading. *Proc. Biol. Sci.* **267**, 1909–1913 (2000).
89. C. Grefkes, P. H. Weiss, K. Zilles, G. R. Fink, Crossmodal processing of object features in human anterior intraparietal cortex: An fMRI study implies equivalencies between humans and monkeys. *Neuron* **35**, 173–184 (2002).
90. J. R. Duhamel, C. L. Colby, M. E. Goldberg, Ventral intraparietal area of the macaque: Congruent visual and somatic response properties. *J. Neurophysiol.* **79**, 126–136 (1998).
91. F. Binkofski *et al.*, Human anterior intraparietal area subserves prehension: A combined lesion and functional MRI activation study. *Neurology* **50**, 1253–1259 (1998).
92. G. R. Fink, R. J. Dolan, P. W. Halligan, J. C. Marshall, C. D. Frith, Space-based and object-based visual attention: Shared and specific neural domains. *Brain* **120**, 2013–2028 (1997).
93. S. Vanni, T. Tanskanen, M. Seppä, K. Uutela, R. Hari, Coinciding early activation of the human primary visual cortex and anteromedial cuneus. *Proc. Natl. Acad. Sci. U.S.A.* **98**, 2776–2780 (2001).
94. H. Horiguchi, S. Nakadomari, M. Misaki, B. A. Wandell, Two temporal channels in human V1 identified using fMRI. *Neuroimage* **47**, 273–280 (2009).
95. C. C. Boucard, J. J. van Es, R. P. Maguire, F. W. Cornelissen, Functional magnetic resonance imaging of brightness induction in the human visual cortex. *Neuroreport* **16**, 1335–1338 (2005).
96. A. Stigliani, B. Jeska, K. Grill-Spector, Encoding model of temporal processing in human visual cortex. *Proc. Natl. Acad. Sci. U.S.A.* **114**, E11047–E11056 (2017).
97. S. Sabbah, M. Worden, D. M. Berson, J. N. Sanes, D. D. Laniado, Code and data - Luxotonic signals in human prefrontal cortex as a possible substrate for effects of light on mood and cognition. Figshare. https://doi.org/10.6084/m9.figshare.c.6054941.v1. Deposited 20 June 2022.
98. S. Sabbah, M. S. Worden, D. D. Laniado, D. M. Berson, J. N. Sanes, Luminance. OpenNeuro. https://doi.org/10.18112/openneuro.ds004065.v1.0.0. Deposited 21 June 2022.